

[Chem. Pharm. Bull.]  
[33(3) 916-926 (1985)]

## Thermal Decompositions of Solid Amino Acids in Relation to Their Hydrogen Bonds. I. Kinetic Studies on the Thermal Decomposition of Solid Cystine

YOSHIHIRO MORI, FUMIKO AKAGI, AKIRA YAJIMA,  
and TAJI KITAGAWA\*

Department of Pharmaceutical Sciences, Toyama Medical and Pharmaceutical  
University, Sugitani, Toyama 930-01, Japan

(Received July 16, 1984)

The solid phase thermal decompositions of L-cystine and its three stereoisomers have been investigated *in vacuo* between 150 and 230 °C. The decomposition processes have been examined by measuring the total pressure and the partial pressures of the four gaseous products, NH<sub>3</sub>, H<sub>2</sub>O, H<sub>2</sub>S, and CO<sub>2</sub>, as well as by the semiquantitative determination of sulfur polymers. The rate equation for the thermal decomposition of L-cystine can be approximated as zeroth order, with an induction period at the initial stage of the decomposition. A remarkable change in the reaction rate was found at around 170–180 °C, above which evaporated sulfur polymers can be detected. At lower temperature the dehydration reaction is predominant, while the rates of formation of NH<sub>3</sub>, H<sub>2</sub>S, and CO<sub>2</sub> become much larger than that of H<sub>2</sub>O as the temperature increases. The observed induction periods at  $T < 200$  °C are different for each of the product gases, and depend strongly on the decomposition temperature and the history of the starting materials. The reactions that occur during this period are discussed. The different behavior observed in the thermal reactions of other sulfur-containing amino acids, L-cysteine and L-methionine, and some non sulfur-containing ones are discussed in relation to the different strengths of the hydrogen bond networks in the crystalline states.

**Keywords**—cystine; cysteine; amino acid; hydrogen bond; thermal decomposition

### Introduction

Most solid amino acids are thermally decomposed to evolve some gaseous products, and small amounts of diketopiperazines, as well as deaminated and decarboxylated compounds and tars are produced.<sup>1-3)</sup> Only a few amino acids such as glycine and aspartic acid are thermally polymerized to form polypeptides.<sup>4-6)</sup> This reaction and related polymerization reactions have been extensively studied to explore the chemical evolution of proteins in prebiotic conditions.<sup>7-8)</sup> Furthermore, some amino acids are known to be sublimed without decomposition when they are heated *in vacuo*.<sup>9)</sup>

The purposes of this series of studies are to investigate these different thermal processes in solid amino acids from the viewpoint of reaction kinetics and to understand them in relation to the energetics and/or orientational properties of the hydrogen bonds formed between the functional groups of each amino acid.

It is well known that two common functional groups of amino acids, -NH<sub>2</sub> and -CO<sub>2</sub>H, can exist in a zwitterion form (NH<sub>3</sub><sup>+</sup> and CO<sub>2</sub><sup>-</sup>) in the crystalline phase.<sup>10)</sup> Those ionic groups are bound to each other *via* three hydrogen bonds of the type N<sup>+</sup>-H···O<sup>-</sup> to form a three-dimensional network. The binding energy between them has been estimated to be about 20 kcal/mol in solid glycine based on measurements of the vapor pressure.<sup>11)</sup> The hydrogen bonds in other amino acids are further strengthened by the contribution of other characteristic groups. In particular, as solid cystine includes two pairs of the ionic groups NH<sub>3</sub><sup>+</sup> and

$\text{CO}_2^-$ ,<sup>12)</sup> its hydrogen bond network is considered to be most rigidly formed. This amino acid also has another reactive group,  $-\text{S}_2-$ . Its role in the thermal decomposition of solid cystine is of great interest since this bond can play an important role in the protection of the biological proteins against physical (thermal or radiational) and chemical perturbations. Fujimaki *et al.* have identified more than ten volatile products in the pyrolysis of cystine and some sulfur-containing amino acids under a nitrogen atmosphere at 200–300 °C.<sup>13–15)</sup> Their results show that the  $-\text{C}-\text{S}_2-$  and  $-\text{S}-\text{S}-$  bonds of cystine are easily dissociated to produce  $\text{H}_2\text{S}$  and  $\text{S}_8$  as well as organic compounds containing one sulfur atom or none.

On the other hand, Seto showed by weight loss measurements with a thermogravimeter that the thermal decomposition of solid L-cystine begins with some intramolecular changes at or above 160 °C and its decomposition occurs rapidly above 210 °C.<sup>16)</sup> Thus, different reactions may occur in different ranges of decomposition temperature.

Olafsson and Bryan have reported the activation energies for the thermal decompositions of several amino acids by the differential scanning calorimetric method.<sup>17)</sup> Their data indicate that sulfur-containing amino acids as well as most basic amino acids decompose with low activation energies. However, little is known about the decomposition kinetics or mechanisms.

In this work, we have first elucidated some mechanistic features in the thermal decompositions of L-cystine and its stereoisomers by the usual method employed in kinetic studies of the thermal decompositions of inorganic solids.<sup>18–21)</sup> The results and some preliminary observations on the thermal processes in other amino acids will be discussed in terms of the different strengths of their hydrogen bond networks.

### Experimental

The thermal decompositions were investigated with evacuation of the gaseous products in order to eliminate secondary reactions as far as possible, because some of the pyrolytic products seem to be formed *via* secondary reactions among the primary products.<sup>14)</sup> The pressure was maintained at  $10^{-3}$ – $10^{-4}$  Torr during the decompositions. Furthermore, such experimental conditions enabled us to observe the sublimation of the starting materials with some amino acids. The decomposition kinetics were studied by measuring the total pressure and the partial pressures of the volatile products. Figure 1 shows the glass apparatus and also the detection systems. Finely powdered or micro crystalline material (0.03–0.4 g) placed in the Pyrex glass cell was dehumidified *in vacuo* at 100 °C for 30–90 min. During such pretreatment of the sample the absorbed water was almost completely removed. Then the material was decomposed with evacuation of the evolved gases at a constant temperature ( $\pm 0.5$  °C) between 150–230 °C, since the decomposition rate above 230 °C was too fast to investigate its kinetics. The decomposition temperature  $T$  was measured by means of a thermocouple soldered on the bottom of the glass cell. As the thermal lag in the cell (1–2 min) was corrected for, the uncertainty in the zero time was within 1 min. The amount of gases evolved in the period required to heat the sample up to  $T$  was found to be negligibly small.

The volatile products were collected in two traps cooled at ice and liquid nitrogen temperatures, respectively. The collected gases were vaporized into a large volume of 1.27 l then passed through an orifice (0.15 mm in diameter) into the ionizer of a quadrupole mass spectrometer (MS) (modified NAG 531, ANELVA). MS were measured in a phase-sensitive way.<sup>22)</sup> The overall sensitivities in the mass spectrometric determinations of  $\text{NH}_3$ ,  $\text{H}_2\text{O}$ ,  $\text{H}_2\text{S}$ , and  $\text{CO}_2$  were corrected by using standard mixtures. With this correction, the relative contents of these gases could be determined

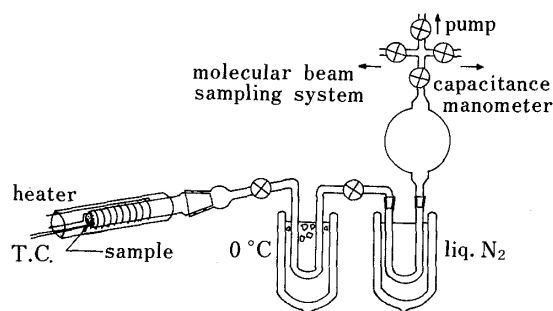


Fig. 1. The Decomposition Cell, and the Collecting and Measuring Systems for Gaseous Products

T.C., thermocouple.

with an error of less than 5% of the observed values. The total pressures were measured with a capacitance manometer (Granville Phillips 212-023).

Thermal decompositions of these materials were also studied by using a high-resolution MS (JMS-D-200, JEOL). In this experiment the sample was heated on a quartz boat used in routine measurements of the MS of low-vapor-pressure solids, and the evolved gases were directly introduced into the ionization chamber. This measurement made it possible to identify some less volatile products such as sulfur polymers, but the absolute amounts could not be determined.

All the materials were obtained from commercial sources. Cystines were recrystallized one or two times from diluted aqueous ammonia solution. The optical purities of cystine isomers were confirmed by measurements of their circular dichroism. The observed  $\Delta\epsilon$  values at 219 nm in 0.1 N HCl were +5.7 and -5.6 for L- and D-cystine, respectively. These values are in agreement with the literature value (+5.9 for L-cystine).<sup>23)</sup>

## Results

### Volatile Products in the Thermal Decompositions of Solid Cystines

The volatile products were mostly collected in the liquid nitrogen trap. By MS determinations, it was found that the bulk of them (>95%) consists of four gaseous products,  $\text{NH}_3$ ,  $\text{H}_2\text{O}$ ,  $\text{H}_2\text{S}$ , and  $\text{CO}_2$ , at the initial stage of the decomposition. A yellowish-brown colored product, possibly sulfur polymers, could also be observed on the inner wall between the upper part of the decomposition cell and the ice trap. Indeed, sulfur polymers could be identified in the experiments by using the high-resolution MS. The observed relative intensities of the sulfur polymer ions were  $\text{S}_2^+$  (2-3) >  $\text{S}_6^+$  (1) >  $\text{S}_5^+$ ,  $\text{S}_4^+$ ,  $\text{S}_3^+$  (ca. 0.5) >  $\text{S}_7^+$ ,  $\text{S}_8^+$  (ca. 0.2) at about 200 °C with an electron energy of 70 eV. This intensity ratio is essentially the same as the result observed for sulfur vapor at the same temperature.<sup>24)</sup> Many other ion peaks were so weak that most of them could not be assigned except for  $\text{HS}_n^+$  and  $\text{H}_2\text{S}_n^+$  ( $n = 1-6$ ), produced by the ionizations of sulfanes  $\text{H}_2\text{S}_n$ .

The numbers of moles of the four gaseous products formed per mole of the starting material ( $N_X^\infty/N_S$ ) were determined after the starting material had been completely decomposed at 195, 213, and 221 °C, where the content of the minor volatile products never exceeded 10% of the total amount of products collected in the liquid nitrogen trap ( $N_T^\infty$ ).

TABLE I. Number of Moles of the Product X per Mole of the Starting Material,  $N_X^\infty/N_S$  ( $X = \text{NH}_3$ ,  $\text{H}_2\text{O}$ ,  $\text{H}_2\text{S}$ ,  $\text{CO}_2$ , and Total), and Fractional Decompositions  $\beta_R$  ( $R = \text{NH}_3^+$ ,  $\text{CO}_2^-$ , and  $-\text{S}_2^-$ ), Obtained from Product Analysis after Complete Decomposition<sup>a)</sup>

	195 °C	213 °C	221 °C
$N_X^\infty/N_S$ X = $\text{NH}_3$	0.57	0.59	$0.61 \pm 0.03^b)$
X = $\text{H}_2\text{O}$	0.50	0.33	$0.28 \pm 0.03$
X = $\text{H}_2\text{S}$	1.1	1.0	$1.0 \pm 0.1$
X = $\text{CO}_2$	0.95	1.0	$1.2 \pm 0.1$
Total	3.5	3.3	$3.4 \pm 0.2$
$N_T^\infty/N_S = (\Sigma(N_X^\infty + \text{others}))/N_S$			
$\beta_{\text{CO}_2^-}^c)$	0.72	0.67	$0.74 \pm 0.08$
$\beta_{\text{NH}_3^+}^d)$	0.54	0.46	$0.45 \pm 0.03$
$\beta_{\text{NH}_3^+}^e)$	0.81	0.71	$0.70 \pm 0.05$
$\beta_{-\text{S}_2^-}^f)$	0.55	0.50	$0.50 \pm 0.05$

a) For the material LA (about 0.04 g); LA is one of the four different materials used in this experiment (see the caption to Fig. 4). b) Average values of three runs. c)  $\beta_{\text{CO}_2^-} = (N_{\text{CO}_2}^\infty + N_{\text{H}_2\text{O}}^\infty)/2N_S$ , obtained by assuming that two  $\text{CO}_2^-$  groups are decomposed into ( $\text{CO}_2 + \text{H}_2\text{O}$ ). d)  $\beta_{\text{NH}_3^+} = (N_{\text{NH}_3}^\infty + N_{\text{H}_2\text{O}}^\infty)/2N_S$ , obtained by assuming that two  $\text{NH}_3^+$  groups are decomposed into ( $\text{NH}_3 + \text{H}_2\text{O}$ ). e)  $\beta_{\text{NH}_3^+} = (N_{\text{NH}_3}^\infty + N_{\text{H}_2\text{O}}^\infty + (N_{\text{H}_2\text{S}}^\infty/2))/2N_S$ , obtained by assuming that the six hydrogen atoms of two  $\text{NH}_3^+$  can contribute to the formation of  $\text{H}_2\text{S}$  as hydrogen (or proton) donors equally well as six hydrogens attached to carbon atoms. f)  $\beta_{-\text{S}_2^-} = N_{\text{H}_2\text{S}}^\infty/2N_S$ .

From the data in Table I it is clear that 70–80% of  $\text{CO}_2^-$  and  $\text{NH}_3^+$  groups and 50–60% of  $-\text{S}_2-$  are decomposed to evolve  $(\text{H}_2\text{O} + \text{CO}_2)$ ,  $(\text{H}_2\text{O} + \text{NH}_3 + \text{H}_2\text{S})$ , and  $\text{H}_2\text{S}$ , respectively. Most of the remaining  $-\text{S}_2-$  could be eliminated as sulfur polymers.

These results of product analysis, though limited to the gaseous products, suggest that the main reactions in the thermal decomposition of solid L-cystine are associated with the evolutions of  $\text{H}_2\text{O}$ ,  $\text{NH}_3$ ,  $\text{H}_2\text{S}$ ,  $\text{CO}_2$ , and sulfur polymers.

### Kinetics

The total pressure ( $P_T$ ) and the partial pressures ( $P_X$ ) of the volatile products were measured as a function of the decomposition time from  $t=0$  to the time ( $t^\infty$ ) when  $P_T$  converged to a constant value ( $P_T^\infty$ ). We first tested the Sharp–Brindley–Achar plots<sup>25)</sup> and the Avrami–Erofeev plots according to the Hancock and Sharp method<sup>26)</sup> to determine the decomposition kinetics. Figure 2 shows the former plot. In these plots the fractional decomposition  $\alpha_T$  derived from  $P_T/P_T^\infty$  was represented as a function of  $t/t_{1/2}^T$ , where  $t_{1/2}^T$  is the time for  $\alpha_T=0.5$ . The slope ( $l$ ) of the latter plot was found to be  $1.15 \pm 0.03$  in the range of  $\alpha_T$  from 0.15 to 0.5 and this value was compared with those derived from various kinds of kinetic equations reported previously. Both plots fit well with those derived from the 2-dimensional phase boundary-controlled interface reaction model (Eq. 1;  $l=1.11$ ).<sup>26,27)</sup>

$$1 - (1 - \alpha_T)^{1/2} = kt \quad (1)$$

However, when  $\alpha_T \geq 0.5$  in Fig. 2, the observed  $\alpha_T$  significantly deviated from Eq. 1, as if the decomposition were decelerated, and the effect was marked at the lower temperature. This deviation should be attributable to subsequent decompositions of the nonvolatile species produced in the initial decomposition, since  $N_T^\infty$  is much larger than  $N_S$  ( $N_T^\infty/N_S = 3.3\text{--}3.5$  at  $T=195\text{--}221^\circ\text{C}$  in Table I). Figure 3 shows the relations of  $\alpha_X$  ( $X=\text{NH}_3$ ,  $\text{H}_2\text{O}$ ,  $\text{H}_2\text{S}$ ,  $\text{CO}_2$ , and total) to the decomposition time. In this figure  $t_{1/2}^X$  for  $X=\text{NH}_3$  is about two times longer than that for  $X=\text{H}_2\text{O}$  and the formation rates of  $\text{H}_2\text{O}$  and  $\text{H}_2\text{S}$  are more markedly

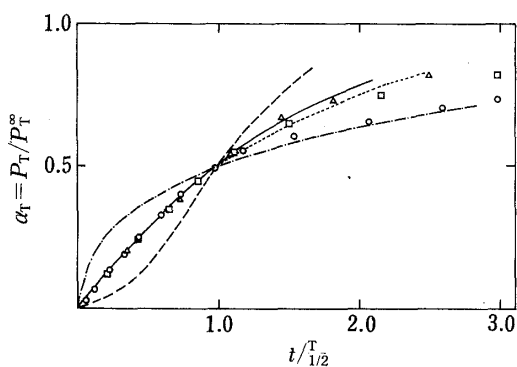


Fig. 2. Determination of Rate Equation According to the Sharp–Brindley–Achar Method

The decomposition data in this work are represented by the following symbols;  $\circ$ — (195°C),  $\square$ — (213°C),  $\triangle$ — (221°C). The characteristic times (min),  $t_{1/2}^T$  and  $t^\infty$ , are (60, 1900), (37, 350), and (21, 250) at 195, 213, and 221°C, respectively.

These plots are compared with those obtained from some kinetic equations reported previously.

-----  $[-\ln(1-\alpha_T)]^{1/2} = kt$  (Avrami–Erofeev Eq. for  $l=2$ )

-----  $[1 - (1 - \alpha_T)^{1/3}]^2 = kt$  (Diffusion-controlled contracting reaction)

—  $1 - (1 - \alpha_T)^{1/2} = kt$  (2-Dimensional phase boundary-controlled contracting interface reaction)

-----  $-\ln(1 - \alpha_T) = kt$  (First-order reaction)

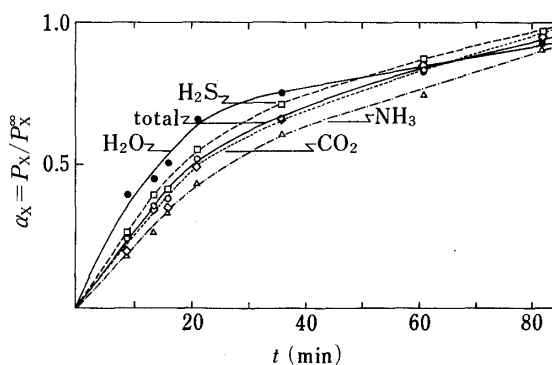


Fig. 3. Thermal Decomposition of Solid L-Cystine at 221°C

The observed times  $t_{1/2}^X$  are  $14 \pm 2$ ,  $18 \pm 1$ ,  $21 \pm 1$ ,  $22 \pm 1$ , and  $26 \pm 1$  min for  $X=\text{H}_2\text{O}$ ,  $\text{H}_2\text{S}$ , total,  $\text{CO}_2$ , and  $\text{NH}_3$ , respectively.

decelerated in the latter part of the decomposition. These results suggest that the nonvolatile products, possibly deaminated and/or decarboxylated and/or desulfurized ones, mainly evolve  $\text{NH}_3$  and  $\text{CO}_2$  in their decompositions, which is clearly different from the decomposition of the starting material, as shown later. In conclusion, the rate Eq. 1 determined by these plots seems not to be very reliable because the fractional decomposition given by  $P_T/P_T^\infty$  or  $P_X/P_X^\infty$  is not necessarily well defined in describing decomposition kinetics including such complicated subsequent decompositions. A more appropriate definition of fractional decomposition, however, could not be provided with our methods of product analysis.

Thus, we next examined the zeroth order rate Eq. 2 containing the apparent fractional decomposition.

$$N_{X(\text{or } T)}/N_S = k_{X(\text{or } T)}(t - t_i^{X(\text{or } T)}) \quad (2)$$

where  $N_{X(T)}$ ,  $k_{X(T)}$ , and  $t_i^{X(T)}$  are the number of moles of the product X or their sum T, the rate constant (mol/(mol of the starting material))  $\cdot \text{s}^{-1}$ , and the induction period for the product X (or T), respectively. This equation was found to be applicable to the initial decompositions below  $N_T/N_S \approx 1.5$  and  $N_X/N_S \approx 0.5-0.6$ . Good fits are apparent in Figs. 4 and 6. From Fig. 4 the average value of  $k_T$  at  $177^\circ\text{C}$  was obtained as  $(6.43 \pm 0.12) \times 10^{-5}$  from more than two runs for material A of L-cystine (abbreviated to LA) with three different values of  $N_S$ . Including the data from the other three materials (LB—LD) the variation of  $k_T$  becomes a little larger  $((6.6 \pm 0.8) \times 10^{-5})$ ; the materials LA—LD differ in their particle forms and sizes, as noted in the figure caption. Also,  $k_X$  ( $X = \text{NH}_3, \text{H}_2\text{O}, \text{H}_2\text{S}$ , and  $\text{CO}_2$ ) varied in the range from 15 to 30% for these materials. Such small material dependences of the rate constants suggest that the main features in the thermal decomposition of L-cystine could be adequately represented by those of the material LA.

The initial decompositions of the other three isomers of cystine obeyed the same rate Eq. 2; but the material dependences were quite large, particularly for the D- and *meso*-isomers

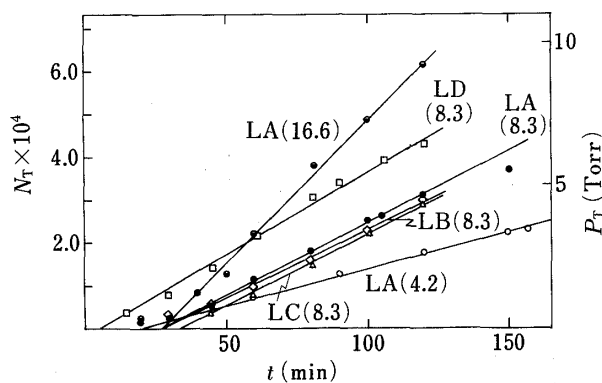


Fig. 4. Dependences of the Thermal Decompositions at  $177^\circ\text{C}$  on Materials (LA—LD) and  $N_S$

The values in the parentheses are  $N_S$  ( $\times 10^{-4}$  mol). LA—LD represent different samples of L-cystine. Material LA ( $\bullet$ ,  $\circ$ ,  $\ominus$ ) consisted of hexagonal plate-like crystals with dimensions of  $50-200 \mu\text{m}$  across and *ca.*  $10 \mu\text{m}$  in thickness, with some fine particles ( $k_T = 6.43 \times 10^{-5}$ ). LB ( $\diamond$ ) was obtained by finely grinding LA in an agate mortar, and had a particle size of  $10-50 \mu\text{m}$  ( $k_T = 5.75 \times 10^{-5}$ ). LC ( $\triangle$ ) had almost the same particle forms and sizes as LA but had been obtained from a different batch of recrystallization ( $k_T = 6.68 \times 10^{-5}$ ). LD ( $\square$ ), prepared by rapid crystallization, had the finest particle size distribution (a few  $\mu\text{m}$ ) ( $k_T = 7.60 \times 10^{-5}$ ).

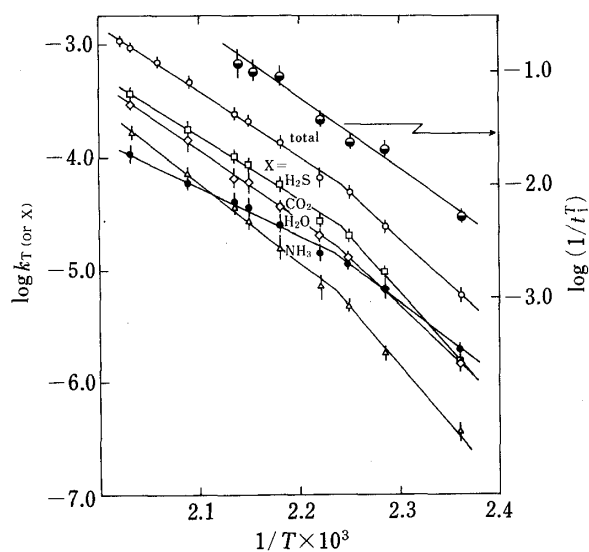


Fig. 5. Arrhenius Plots for the Rate Constants in the Thermal Decomposition of L-Cystine (Material LA)

(100—200% for  $k_T$ ) and also in the initial decomposition of DL-cystine, as discussed later. The obtained  $k_T$  for DL-cystine was nearly equal to or a little larger than that of L-cystine at each temperature.

### Activation Energies and Formation of Sulfur Polymers

The Arrhenius plots for  $k_T$  and  $k_X$  are presented in Fig. 5. These plots show the existence of two straight lines with different activation energies above and below 170—180 °C. The activation energies and the preexponential factors obtained from Fig. 5 are given in Table II. The activation energies  $E_X$  in the higher temperature range increase in the following order.

$$E_{\text{H}_2\text{O}} < E_{\text{H}_2\text{S}} < E_{\text{CO}_2} < E_{\text{NH}_3}$$

Olafsson and Bryan have previously obtained the activation energy in the pyrolysis of solid L-cystine in the temperature range from 230 to 270 °C by using a differential scanning calorimeter. Their value (32.7 kcal/mol) is significantly larger than  $E_T$  (27.7 kcal/mol) obtained in this work, and rather near  $E_{\text{NH}_3}$  (30.5 kcal/mol). This is consistent with the extrapolated results based on the parameters in Table II that the formation reaction of  $\text{NH}_3$  as well as that of  $\text{CO}_2$  having larger activation energies becomes predominant at  $T > 250$  °C.

The characteristic temperature (170—180 °C) observed in the decomposition rates was found to correspond to the temperature above which the evaporated sulfur polymers were detected in another experiment using the high-resolution MS. The total intensity of  $\text{S}_n^+$  ( $n = 2-8$ ) at 220 °C is 3—4 times that at 190 °C. This increase qualitatively accords with the increase of the vapor pressure of solid sulfur,<sup>28)</sup> and then it corresponds to the largest decrease in  $E_{\text{H}_2\text{S}}$  (ca. 23 kcal/mol in Table II) above 170—180 °C, that is, the formation rate of  $\text{H}_2\text{S}$  apparently decreases as the decomposition temperature increases. Therefore it can be concluded that the formation of  $\text{H}_2\text{S}$  competes with the evaporation of sulfur polymers above 170—180 °C.

### Induction Periods

The induction periods ( $t_i^X$ ) were determined according to Eq. 2 by the least-squares method, so the uncertainties are estimated to be 10—20% of  $t_i^X$ . Besides,  $t_i^X$  was obtained for  $N_S \geq 8.3 \times 10^{-4}$  mol (=0.20 g) because  $t_i^X$  slightly depends on  $N_S$  for  $N_S < 8.3 \times 10^{-4}$  mol as shown in Fig. 4.

The observed induction periods in L-cystine are different for each of the products X and depend strongly on the decomposition temperature and the history of the materials. Figure 6 shows an example of the dependences of  $t_i^X$  on the products X. Above 180 °C,  $t_i^X$  for  $X = \text{NH}_3$ ,  $\text{H}_2\text{S}$ , and  $\text{CO}_2$  are almost equal but  $t_i^{\text{H}_2\text{O}}$  is nearly zero, whereas below 180 °C the dehydration reaction also requires some induction period, though it is shorter than those for the other

TABLE II. Activation Energies and Preexponential Factors in the Thermal Decomposition of Solid L-Cystine<sup>a)</sup>

X	Above 170—180 °C		Below 170—180 °C	
	$E_X$ (kcal/mol)	$\log A_X^b$	$E'_X$ (kcal/mol) <sup>c)</sup>	$\Delta E = E'_X - E_X^c)$
$\text{NH}_3$	$30.5 \pm 0.8$	$10.6 \pm 0.2$	46	15
$\text{H}_2\text{O}$	$18.6 \pm 0.7$	$4.8 \pm 0.1$	33	14
$\text{H}_2\text{S}$	$24.4 \pm 0.1$	$8.1 \pm 0.1$	47	23
$\text{CO}_2$	$27.5 \pm 0.8$	$9.5 \pm 0.3$	41	13
Total	$27.7 \pm 0.5$	$9.2 \pm 0.2$	37	9

a) For the material LA. b) (mol per mol of L-cystine) · s<sup>-1</sup>. c) The uncertainties are estimated to be  $\pm 3-5$  kcal/mol.

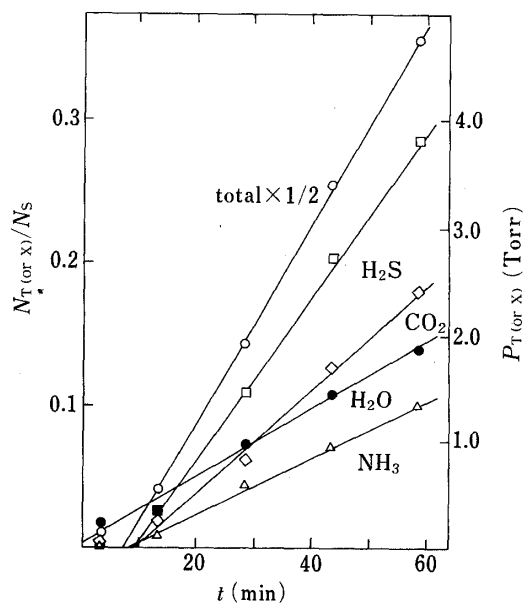


Fig. 6. Induction Periods of the Gaseous Products X at 195 °C

The obtained  $t_i^X$  are 7, 8, 0, 9, and 9 min for X=total, NH<sub>3</sub>, H<sub>2</sub>O, H<sub>2</sub>S, and CO<sub>2</sub>, respectively.

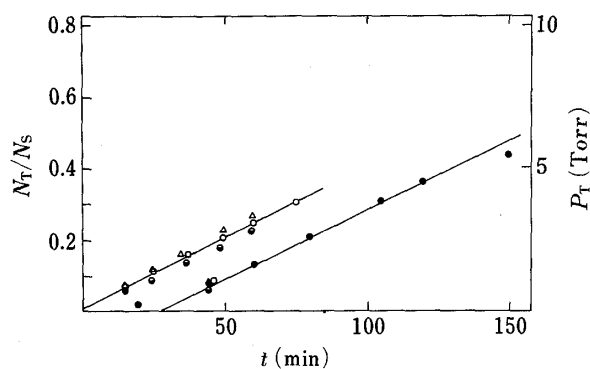


Fig. 7. Irreversible Change after the Induction Period at 177 °C

Material LA ( $N_S=8.3 \times 10^{-4}$  mol), which should decompose along the lines (—●—) as indicated in Fig. 4, was decomposed for about 45 min at 177 °C, and then cooled at room temperature *in vacuo*. Then, it was decomposed again at the same temperature without further treatment (—○—) or after a 1 h exposure to air (—△—) or a 4.5 h exposure to water vapor (15 Torr) (—●—).

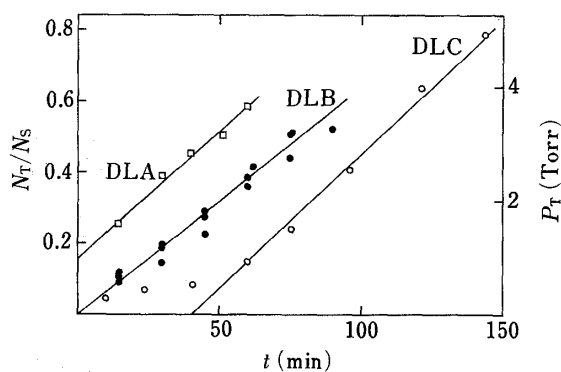


Fig. 8. Material Dependences of the Decomposition Behavior of DL-Cystine at 180 °C ( $N_S=4.2 \times 10^{-4}$  mol)

All the materials, DLA (—□—), DLB (—●—), and DLC (—○—), are powder-like ones having very fine particles (a few  $\mu\text{m}$ ) together with small aggregates.

three gases at each temperature. In general, the induction periods increase in the following order.

$$t_i^{\text{H}_2\text{O}} < t_i^{\text{NH}_3} \approx t_i^{\text{CO}_2} \leq t_i^{\text{H}_2\text{S}}$$

The materials decomposed for a certain time longer than  $t_i^T$  at each temperature then cooled and subsequently decomposed again at the same temperature no longer showed any induction period, as shown in Fig. 7. Furthermore, the material phase formed after the induction period was found to be unaffected by exposure to air or water vapor.

Material dependences of the induction periods were observed in the four isomers of cystine, particularly in DL-cystine, as shown in Fig. 8. DLA and DLB have an apparently "negative" and zero induction period, respectively, in spite of having almost the same rate constants. These phenomena were found by product analysis to arise from the rapid

evolutions of both  $\text{CO}_2$  and  $\text{NH}_3$  at the initial stage of decomposition. These initial formations of  $\text{CO}_2$  and  $\text{NH}_3$  could be depressed when absorbed water was incompletely removed before the decomposition. The induction period for the formation of  $\text{H}_2\text{S}$ , however, was always positive and independent of such pretreatment of the materials. Its material dependence is rather small in all four isomers. One possible source to produce  $\text{CO}_2$  and  $\text{NH}_3$  initially is considered to be some surface or crystal imperfections with an incomplete hydrogen bond network between  $\text{NH}_3^+$  and  $\text{CO}_2^-$ , which are protected by the absorbed water. Such imperfections may be more easily formed when the DL-isomer is recrystallized as a racemic compound.<sup>29)</sup> Related phenomena due to imperfections or different crystal structures in solid cystine isomers have been briefly reported by others.<sup>30,31)</sup>

## Discussion

### Initial Decompositions

The findings concerning the induction periods lead us to several conclusions regarding the initial reactions that occurred during or immediately after these periods:

(1) The main reaction determining the length of the induction period is strongly related to the evolution of  $\text{H}_2\text{S}$ .

(2) The dehydration reaction precedes this reaction.

(3) The evolutions of  $\text{CO}_2$  and  $\text{NH}_3$  occur almost together with that of  $\text{H}_2\text{S}$ , although there are some exceptional cases depending on the properties of the starting materials.

Based on these results, the following reactions are considered to take place in the initial decomposition of solid cystines.

The dehydration reaction precedes all other reactions which can be probed by detecting the volatile products. However, this does not necessarily rule out some physical or chemical changes which do not produce any gaseous species before the dehydration reaction is initiated, because there is some induction period for the evolution of  $\text{H}_2\text{O}$  at lower temperatures. The dehydration reaction should be associated with the partial destruction of the hydrogen bond network formed between  $\text{NH}_3^+$  and  $\text{CO}_2^-$ . This would cause an increase of free or incompletely hydrogen-bonded  $\text{NH}_3^+$  and  $\text{CO}_2^-$  groups, from which both  $\text{NH}_3$  and  $\text{CO}_2$  could easily be produced, leading to their rapid evolutions at a very early stage in the decomposition of DL-cystine, for example.

It is likely that the C-S and/or S-S bonds are dissociated as early as the stage at which the dehydration reaction occurs. Indeed, Fujimaki *et al.* detected small amounts of some desulfurized amino acids such as alanine, leucine, and methionine after the pyrolysis of solid cystine for only 1 min at 270–300 °C.<sup>14)</sup> The dissociations of these bonds could also eliminate atomic S or  $\text{S}_2$ , which could be partially polymerized as they diffuse toward the surface through the two dimensional arrays of  $(-\text{S}_2-)$  in the crystalline state. Such a polymerization process of sulfur may correspond to the chain reaction mechanism in the pyrolytic formation of elementary sulfur from episulfides.<sup>32)</sup> Thus, sulfur polymers can be gradually grown over the surface and/or the interface of the polycrystalline materials during the induction period.

The gaseous product  $\text{H}_2\text{S}$  is presumably produced by the reduction of these sulfur polymers. This mechanism could reasonably explain the formation of sulfanes  $\text{H}_2\text{S}_n$ .

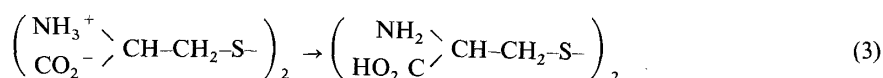
### Relation to the Hydrogen Bond Strength

It is of interest to compare these thermal decomposition reactions in solid cystines with those in other sulfur-containing amino acids, L-cysteine and L-methionine. These two amino acids were found to have very rapid sublimation rates, whereas solid cystines were decomposed with no sublimation. Namely, 80% of the starting material of L-cysteine and 100% of L-methionine were sublimed at 192 °C after 90 min. The remaining L-cysteine was



decomposed to evolve  $\text{NH}_3$ ,  $\text{H}_2\text{O}$ ,  $\text{H}_2\text{S}$ , and  $\text{CO}_2$ . The relative amounts of products (0.66 : 0.37 : 1.0 : 0.85) were almost the same in the case of L-cystine (0.50 : 0.33 : 1.0 : 0.83). Sulfur polymers were detected in the case of L-cysteine, too. Therefore the thermal decomposition of solid L-cysteine seems to proceed like those of cystines.

Such differences in the thermal reactions of these three amino acids can be understood in terms of the different strengths of the intermolecular hydrogen bonds in the solids as follows. Two ionic pairs of  $\text{NH}_3^+$  and  $\text{CO}_2^-$  of a cystine molecule are known to interact strongly through 6 ( $\text{N}^+-\text{H}\cdots\text{O}^-$ ) hydrogen bonds between neighboring molecules with an average distance of 2.82 Å.<sup>12,33</sup> The total energy of these hydrogen bonds ( $E_{\text{HB}}$ ) is estimated to be  $45 \pm 5$  kcal/mol if we assume 4–5 kcal/mol per hydrogen bond between  $\text{N}-\text{H}\cdots\text{O}$  with a distance of about 2.8 Å,<sup>10,11,34</sup> and 15–20 kcal/mol for the transfer energy of two protons as represented in Eq. 3.<sup>11</sup> The heat of sublimation can be estimated to be  $55 \pm 5$  kcal/mol by



adding the van der Waals energy (7–10 kcal/mol)<sup>35</sup> to  $E_{\text{HB}}$ . This is approximately twice the heat of sublimation of glycine (31.2 kcal/mol).<sup>11</sup> This energy is much larger than all the observed activation energies, but is comparable with the bond energy between  $-\text{C}-\text{S}_2-$  (55 kcal/mol) or a little smaller than that of  $\text{CS}-\text{CS}$  (70–75 kcal/mol).<sup>36</sup> Therefore the thermally activated L-cystine molecules are expected to be decomposed by the dehydration reaction having the smallest activation energy and by the dissociation of the comparatively weak central bonds ( $\text{C}-\text{S}$  and  $\text{S}-\text{S}$ ) before they are sublimed as free molecules. In L-methionine, only three ( $\text{N}^+-\text{H}\cdots\text{O}^-$ ) hydrogen bonds exist.<sup>37</sup> The hydrogen bond energy (20–25 kcal/mol) is as small as the activation energies for the dehydration reaction obtained in L-cystine (18.6 and *ca.* 33 kcal/mol), so the molecule can be expected to sublime quite readily. L-Cysteine is an intermediate case with  $E_{\text{HB}} = 25$ –30 kcal/mol, where the molecules interact with each other through 3 ( $\text{N}^+-\text{H}\cdots\text{O}^-$ ) hydrogen bonds and two weak hydrogen bonds between  $\text{S}-\text{H}$  and  $\text{S}$  or  $\text{O}^-$ .<sup>38</sup>

Similar relations of the hydrogen bonds to the thermal changes can be found in other amino acids, too. According to the results reported by Gross and Grodsky,<sup>9</sup> most amino

TABLE III. Thermal Decompositions of Solid Amino Acids in Competition with Sublimation

Amino acid	Gross <i>et al.</i>		$N_T/N_S^c$	This work <sup>a)</sup>			
	D or S <sup>b)</sup>			Relative content			
				$\text{H}_2\text{O}$	$\text{NH}_3$	$\text{CO}_2$	$\text{H}_2\text{S}$
Cystine	D	D	1.1	0.33	: 0.50	: 0.83	: 1.0
Glu	D	D <sup>d)</sup>	0.94	1.0	: 0.02	: 0.01	
Arg	D	D	0.13	1.0	: 1.2	: 0.01	
Lys	D	D	0.45	1.0	: 0.1	: 0.03	
Asp	D (S)	D	0.47	1.0	: 0.03	: 0.03	
Ser	D (S)	S (D)	0.1	1.0			
His	D (S)	D	0.01	1.0			
Cys	S (D)	S (D)	0.14	0.37	: 0.66	: 0.85	: 1.0
Thr	S (D)	S (D)	0.01	1.0			
Met	S	S	0.0				

a) Samples of about 0.2 g were decomposed at 192–195°C for 90 min. b) D, decomposed; D (S), decomposed with a little sublimation; S (D), sublimed with a little decomposition; S, sublimed. c) Fractional decomposition is given by the total number of moles of gaseous products ( $N_T$ ) per mole of the starting material ( $N_S$ ). d) The dehydrated product is sublimed.

acids with only three ( $\text{N}^+-\text{H}\cdots\text{O}^-$ ) hydrogen bonds can be sublimed with no decomposition. On the other hand, the amino acids having additional hydrogen bonds other than these three bonds tend to decompose with no sublimation or in competition with sublimation.

Our preliminary results on the thermal decompositions of these amino acids are also in accord with their results, as given in Table III. In the table, the relative ratios of the gaseous products and the approximate fractional decompositions,  $N_T/N_S$ , were determined after decomposition at 192–195 °C for 90 min. The major product was found to be  $\text{H}_2\text{O}$  in all cases. The evolution of  $\text{NH}_3$  was also observed in the decompositions of arginine and lysine, which contain a guanidyl group and one more amino group, respectively. However, only a little  $\text{CO}_2$  could be detected at the above temperature. Therefore it appears that the dehydration reaction is generally the most important one in their thermal decompositions. Further investigations on the decomposition processes should enable us to relate them to the properties of the hydrogen bond networks in the solid amino acids.

**Acknowledgement** The authors wish to thank Mr. M. Morikoshi and Mr. K. Niino for measurements of high-resolution MS and Dr. K. Mawatari for measurements of circular dichroism. Thanks are also due to Dr. H. Shinoda for helpful discussions. This research was supported in part by a Grant-in-Aid for Scientific Research from the Ministry of Education, Science and Culture, Japan.

#### References and Notes

- 1) E. Katchalski, *Adv. Protein Chem.*, **6**, 123 (1951).
- 2) E. G. Curphey, *Chem. Ind. (London)*, **1956**, 783.
- 3) M. A. Ratcliff, E. E. Medley, and P. G. Simmonds, *J. Org. Chem.*, **39**, 1481 (1974).
- 4) A. B. Maggy, *J. Chem. Soc.*, **1954**, 1444.
- 5) J. Kovacs and I. Konyves, *Naturwissenschaften*, **43**, 333 (1954).
- 6) A. Vegotsky, K. Harada, and S. W. Fox, *J. Am. Chem. Soc.*, **80**, 3361 (1958).
- 7) K. Harada and S. W. Fox, *J. Am. Chem. Soc.*, **80**, 2694 (1958).
- 8) S. W. Fox, *Nature (London)*, **23**, 328 (1965).
- 9) D. Gross and J. Grodsky, *J. Am. Chem. Soc.*, **77**, 1678 (1955).
- 10) T. F. Koetzle and M. S. Lehmann, "The Hydrogen Bond/II" ed. by P. Schuster, G. Zundel, and C. Sandorfy, North-Holland, Amsterdam, 1976, Chapt. 9.
- 11) S. Takagi, H. Chihara, and S. Seki, *Bull. Chem. Soc. Jpn.*, **32**, 84 (1959).
- 12) B. M. Oughton and P. M. Harrison, *Acta Crystallogr.*, **12**, 396 (1959).
- 13) N. Kobayashi and M. Fujimaki, *Agric. Biol. Chem.*, **29**, 191 (1965).
- 14) M. Fujimaki, S. Kato, and T. Kurata, *Agric. Biol. Chem.*, **33**, 1144 (1969).
- 15) S. Kato, T. Kurata, S. Ishiguro, and S. Fujimaki, *Agric. Biol. Chem.*, **37**, 1759 (1973).
- 16) J. Seto, *Bunseki Kagaku*, **9**, 939 (1960).
- 17) P. G. Olafsson and A. M. Bryan, *Polymer Letters*, **9**, 521 (1971).
- 18) P. W. M. Jacobs and A. R. T. Kureishy, *Trans. Faraday Soc.*, **58**, 551 (1962).
- 19) P. W. M. Jacobs and H. M. Whitehead, *Chem. Rev.*, **69**, 551 (1969).
- 20) E. Ellsworth and H. C. Beachell, *J. Phys. Chem.*, **76**, 3545 (1972).
- 21) H. F. Cordes and S. R. Smith, *J. Phys. Chem.*, **72**, 2189 (1968).
- 22) Y. Mori, T. Kitagawa, T. Yamamoto, K. Yanada, and S. Nagahara, *Bull. Chem. Soc. Jpn.*, **53**, 3492 (1980).
- 23) M. Legrand and R. Viennet, *Bull. Chem. Soc. France*, **1965**, 679.
- 24) J. Berkowitz and J. R. Marquart, *J. Chem. Phys.*, **39**, 275 (1963).
- 25) J. H. Sharp, G. W. Brindley, and B. N. N. Achar, *J. Am. Ceram. Soc.*, **49**, 379 (1969).
- 26) J. D. Hancock and J. H. Sharp, *J. Am. Ceram. Soc.*, **55**, 74 (1972).
- 27) K. L. Mampel, *Z. Phys. Chem.*, **A187**, 43, 235 (1940).
- 28) B. Meyer, *Chem. Rev.*, **76**, 381 (1976).
- 29) M. Delfino, *Mol. Cryst. Liq. Cryst.*, **52**, 272 (1979).
- 30) H. Shields and P. J. Hamrick, *J. Chem. Phys.*, **64**, 263 (1964).
- 31) H. E. Van Wart and H. A. Scheraga, *J. Phys. Chem.*, **80**, 1812 (1976).
- 32) O. P. Strausz, H. E. Cuning, and J. W. Lown, "Chemical Kinetics," Vol. 5, Elsevier, Amsterdam, 1972, Chapt. 6.
- 33) M. O. Chaney and L. K. Steinrauf, *Acta Crystallogr., Sect. B*, **30**, 711 (1974).
- 34) G. C. Pimentel and A. L. McClellan, "The Hydrogen Bond," W. H. Freeman, San Francisco, 1960.

- 
- 35) The van der Waals energy between neutral cystine molecules can be estimated from the heat of sublimation of related C<sub>8</sub>-C<sub>10</sub> compounds, obtained from T. Boublick, and F. E. Hala, "The Vapour Pressures of Pure Substances," Elsevier, Amsterdam, 1973.
  - 36) S. W. Benson, *Chem. Rev.*, **78**, 23 (1978).
  - 37) K. Torii and Y. Iitaka, *Acta Crystallogr., Sect. B*, **29**, 2799 (1973).
  - 38) K. A. Kerr, J. P. Ashmore, and T. F. Koetle, *Acta Crystallogr., Sect. B*, **31**, 2022 (1975).